JOC The Journal of Organic Chemistry

Article

pubs.acs.org/joc

1,3,6,8-Tetraazapyrenes: Synthesis, Solid-State Structures, and Properties as Redox-Active Materials

Sonja Geib,[†] Susanne C. Martens,[†,§] Ute Zschieschang,[‡] Florian Lombeck,[†] Hubert Wadepohl,[†] Hagen Klauk,[‡] and Lutz H. Gade*[,†]

[†]Anorganisch-Chemisches Institut, Universität Heidelberg, Im Neuenheimer Feld 270, D-69120 Heidelberg, Germany

[‡]Max Planck Institute for Solid State Research, Heisenbergstrasse 1, D-70569 Stuttgart, Germany

Supporting Information

ABSTRACT: A series of new tetraazapyrene (**TAPy**) derivatives has been synthesized by reducing 1,4,5,8-tetranitronaphthalene to its corresponding tin salt (**I**) and reacting it with perfluorinated alkyl or aryl anhydrides. The resulting 2,7-disubstituted **TAPy** molecules and the known parent compound 1,3,6,8-tetraazapyrene (**II**) have been further derivatized by core chlorination and bromination. The brominated compounds served as starting materials for Suzuki cross-coupling reactions with electron-poor arylboronic acids. Single-crystal X-ray analyses established polymorphism for some **TAPy** compounds. The ground-state geometries of all new **TAPy** derivatives were modeled with DFT methods [B3PW91/6-31 g(d,p) and B3PW91/6-311+g(d,p)], especially focusing on the energies of the lowest unoccupied molecular orbital (LUMO) and the electron affinities (EA) of the molecules. The results of the calculations were confirmed experimentally by cyclic voltammetry to evaluate the substitution effects at the 2 and 7 position and the core positions, respectively, and gave LUMO energy levels that range from −3.57 to −4.14 eV. Fabrication of organic field-effect transistors (OFETs) with several of these tetraazapyrenes established their potential as organic n-type semiconductors.

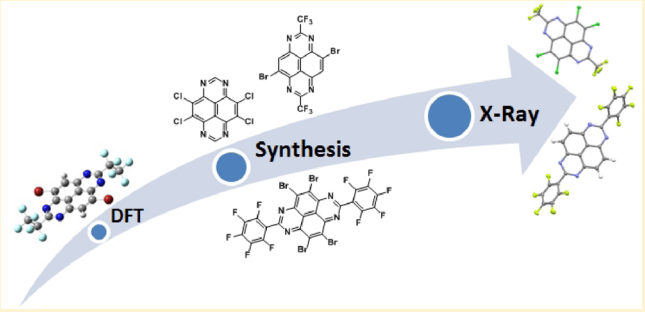

INTRODUCTION

During the past decade, there has been growing interest in developing new organic, π-conjugated materials[1] for application in electronic and optoelectronic devices, such as light-emitting diodes (LEDs), field-effect transistors (FETs), and solar cells.[2,3] We recently studied a new class of polyheterocyclic aromatics, 1,3,8,10-tetraazaperopyrenes (**TAPPs**)[4,5] and established their use either as functional dyes or n-type semiconductors in the field of organic electronics.[6] Inspired by the interesting results obtained with this class of azaaromatic compounds we decided to investigate a similar class of polycyclic aromatics, 1,3,6,8-tetraazapyrenes (**TAPys**), which can be seen as "contracted" **TAPPs**, containing one naphthalene core unit less. By reducing the size of the aromatic core, not only the solubility of the molecules in organic solvents but also the options of derivatization were thought to be enhanced. By variation of the substituents at the 2 and 7 position as well as at the aromatic core the electronic properties were expected to be specifically influenced. For example, introduction of perfluorinated substituents as well as halogens are known to lower the LUMO energy levels significantly, making such tetraazapyrene derivatives interesting candidates for n-channel semiconducting materials that might be processable from solution.

The parent compound, 1,3,6,8-tetraazapyrene, was first described in 1927 by Dimroth and Roos, but initially its physical properties remained unexplored and no derivatives were prepared.[7] It was not until 1964 that the synthesis of two derivatives, 2,7-dimethyl- and 2,7-diphenyl-1,4,6,8-tetraazapyrene, was published and the EPR spectra of the corresponding radical cation and anion were studied in detail.[8,9] Three patents describe the synthesis of several 2,7-dialkyl substituted as well as halogenated 1,3,6,8-tetraazapyrenes which were claimed to possess pharmaceutical activity against protozoan infections.[10] Pozharskii and co-workers synthesized 2,7-dimethyl-1,3,6,8-tetraazapyrene starting from 6,7-dinitro-2-methylperimidine[11] and Aksenov et al. recently published an alternative synthetic way to obtain inter alia 2,7-dimethyl- and 2,7-diphenyltetraazapyrenes from pyrimidine ketones.[12] Apart from these few examples, tetraazapyrenes have been unexplored to date.

In this work, we report a general method for the synthesis of 2,7-perfluoroalkyl-substituted tetraazapyrenes as well as several methods for the core-substitution of different derivatives, including bromination and chlorination procedures, which then again give access to versatile building blocks for further conversions of these compounds in Suzuki cross-coupling reactions. Furthermore, we present a detailed study of the redox properties of the **TAPy** derivatives and a first investigation into the performance of some **TAPys** as organic semiconducting materials in n-channel thin-film transistors (TFTs).

Received: May 3, 2012
Published: June 25, 2012

dx.doi.org/10.1021/jo300894p | J. Org. Chem. 2012, 77, 6107−6116

RESULTS AND DISCUSSION

Synthesis. The parent compound, 1,3,6,8-tetraazapyrene (**II**), which was subsequently used as starting material, was synthesized according to literature procedure by reducing 1,4,5,8-tetranitronaphthalene[13] with tin dust in fuming hydrochloric acid and subsequent cyclization with formic acid.[7,14] Core substitution of **II** could be achieved by classical chlorination and bromination methods. For the introduction of chlorine substituents, **II** was dissolved in chlorosulfonic acid and reacted with chlorine gas in the presence of catalytic amounts of iodine to yield compound **1a** (Scheme 1). The corresponding brominated **TAPy** (**1b**) was synthesized accordingly by direct bromination of **II** in concentrated sulfuric acid (Scheme 1).

Scheme 1. Synthesis of 1,3,6,8-Tetraazapyrene (II) and Its Tetrahalogenated Derivatives 1a and 1b

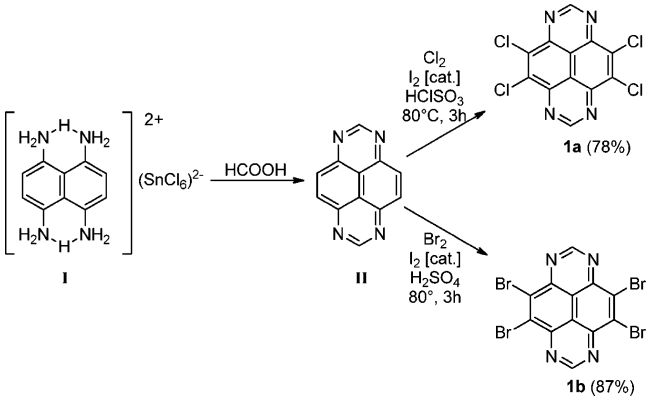

For the introduction of substituents in the positions 2 and 7 a preparative method, based on synthetic procedures developed for known **TAPy**[9,10] and **TAPP**[6] derivatives, was employed. The synthesis of the 2,7-bisperfluoroalkyl-1,3,6,8-tetraazapyrenes (**2a**–**c**) and 2,7-bispentafluorophenyl-1,3,6,8-tetraazapyrene (**3**) was achieved by reducing 1,4,5,8-tetranitronaphthalene[13] as described above to the corresponding ammonium/tin(II) salt[14] (**I**), followed by the addition of an excess of the corresponding perfluoroalkyl- or perfluorophenyl carboxanhydrides in refluxing THF in the presence of catalytic amounts of triethylamine to generate the free tetraamino species (Scheme 2a). Column chromatography and recrystallization from methanol gave the desired products **2a**–**c** and **3** in moderate yields of 36–63% as light yellow solids (Scheme 2a). The relatively low yields are due to as yet incompletely understood side reactions which give rise to several minor components.

In contrast to the case of the parent compound **II**, the core-halogenation of the 2,7-bis(perfluoralkylated) **TAPy**s was not achieved as easily because of the electron withdrawing nature of the substituents. In order to obtain core-brominated 2,7-bis(perfluoralkyl)-substituted **TAPy** derivatives, **2a**–**c** were reacted with dibromoisocyanuric acid (DBI)[15] in concentrated sulfuric acid (Scheme 2b). Remarkably, only the 2-fold brominated **TAPy** derivatives **4a**–**c** (Scheme 2b) were isolated, and no traces of higher substituted reaction products were observed even though a large excess (8 equiv) of DBI was employed. Tetraazapyrenes **4a**–**c** were obtained as colorless to light yellow solids after extraction with dichloromethane and recrystallization from methanol. For 2,7-bisperfluorophenyl-**TAPy 3** the same reaction conditions only gave mixtures of two- to 4-fold brominated derivatives which could not be separated. However, in this particular case bromination with bromine in concentrated sulfuric acid could be applied selectively giving the tetrabrominated product **5** (Scheme 2b). Apparently, the deactivation of the aromatic system caused by the perfluorinated phenyl substituent does not inhibit the classical bromination method. The yield, however, is significantly lower (18%) than for **1b** (87%).

Core-chlorination of the 2,7-disubstituted **TAPy**s turned out to be a greater challenge and was eventually only successfully carried out for derivative **2a** (Scheme 2b). While the 4-fold chlorination of 2,9-perfluoroalkyl-substituted tetraazaperopyrene (**TAPP**) derivatives is selectively achieved with dichloroisocyanuric acid (DCI),[16] as we have presented recently,[6] the conversion of **2a** with DCI not only results in a mixture of the 1-, 2-, 3- and 4-fold substituted compounds with low yields but also requires more drastic conditions and significantly longer reaction times. However, the 4-fold substituted derivative **6** (Scheme 2b) could be isolated as the main product after reacting **2a** with ten equivalents of DCI in concentrated sulfuric acid at 100 °C for 10 days. Even though the yield of 13% is not significantly lower than for compound **5** (18%), it is important to note that the formation of **6** as the main product could only be observed when the reaction was carried out on a small scale.

Further derivatization was achieved by Suzuki cross-coupling. Due to the fact that bromides are known to be more reactive in these transformations than their chlorinated analogues[17] and since they were easier to obtain, compounds **1b** and **4a** were chosen as starting materials for the following conversions. In order to obtain molecules with low LUMO energy levels, two boronic acids with electron withdrawing groups in their *para*-position were chosen for the cross-coupling reaction: *p*-cyanophenylboronic acid and *p*-trifluoromethylphenylboronic acid. Using $Pd(dppf)Cl_2$ as catalyst gave the desired cross-coupling target molecules **7a**,**b** and **8a**,**b** (Scheme 3).

Crystal Structures. Since tetraazapyrenes (**TAPys**) were thought to potentially display semiconducting properties, it was of interest to study their packing behavior in the solid state which strongly influences charge-carrier mobilities and stability and thus the performance of organic semiconducting devices. Recent literature discusses molecular packing motifs that are favorable for achieving high charge-carrier mobilities.[2k,18,19] Among these motifs, especially a 2-D-π-stacking or at least a 1-D-π-stacking should be present in the solid state in order to enable an efficient charge transport. On the other hand, herringbone patterns (with or without π-overlap) are commonly associated with low or no conductivity.[2k,18,19]

The crystal and molecular structures of several **TAPy** derivatives have been determined. The molecular structures are characterized by the planar tetraazapyrene core with almost identical bond lengths and angles (see the Supporting Information) with either the two perfluoroalkyl substituents pointing in opposite directions above and below (**2b**–**c**, **4b**) or the phenyl substituents being rotated out of the plane of the polycyclic molecular core to reduce the steric repulsion (**3**, **5**), respectively.

More importantly, a variety of motifs have been observed for the packing pattern of **TAPy** molecules (Table 1). Apart from the obvious influence of substitution, the organic solvent from which the crystals were grown also has an impact, as has been shown by the crystallization of different polymorphic solvent-free forms of **2a** and **2c** and by the formation of crystal solvates, such as **3**·THF and **5**·2 toluene (Table 1).

dx.doi.org/10.1021/jo300894p | J. Org. Chem. 2012, 77, 6107–6116

Scheme 2. Synthesis of the (a) 2,7-Disubstituted 1,3,6,8-Tetraazapyrenes 2a–c and 3 and (b) Their Core-Brominated Derivatives 4a–c and 5 and the Core-Chlorinated Derivative 6

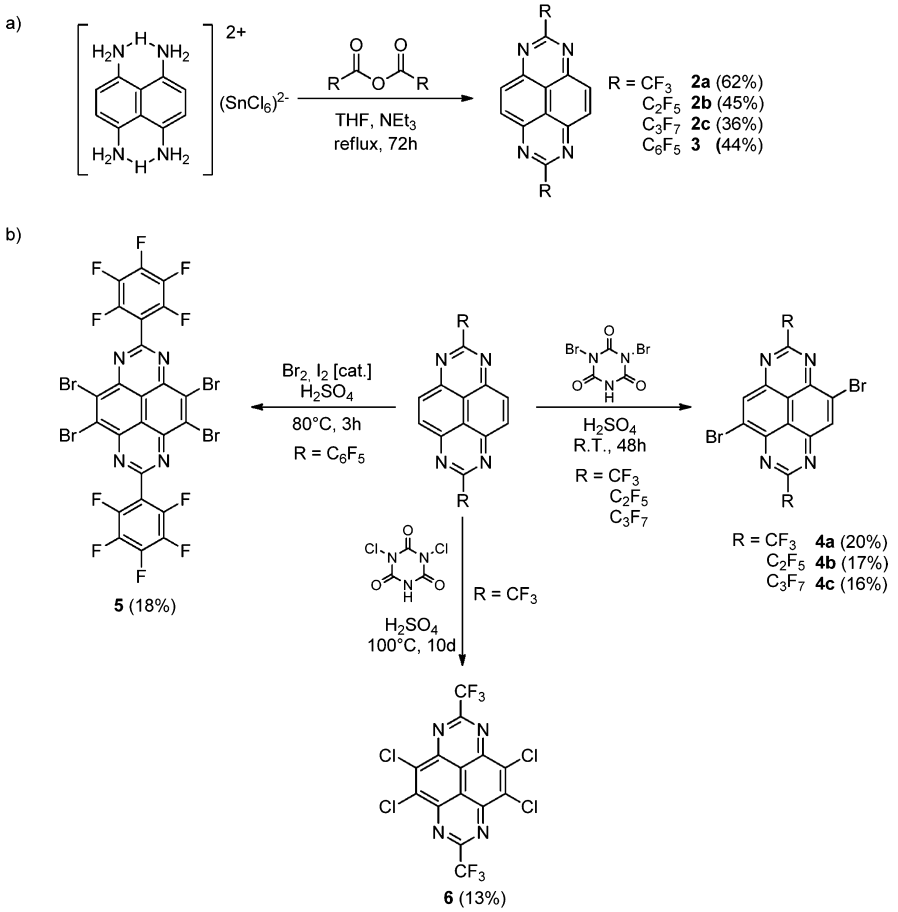

Scheme 3. Suzuki Cross-Coupling of the Core-Brominated TAPy Derivatives 1b and 4a with Arylboronic Acids

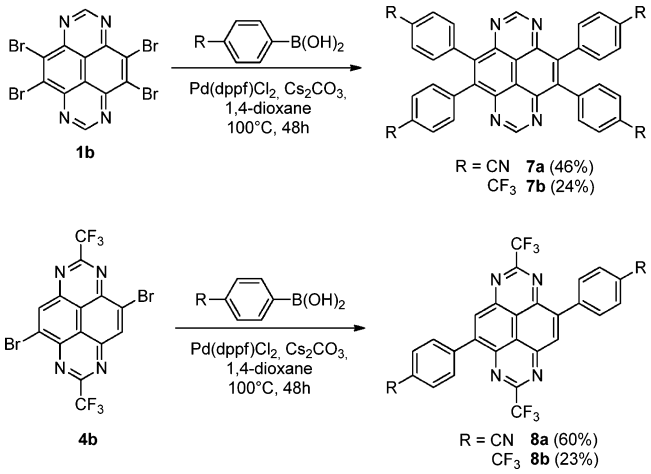

The packing pattern in the monoclinic modification of **2a** is dominated by two separate layers of $\pi-\pi$-stacks with the two stacks being rotated by 86° with respect to each other. The interplanar distance between the polycyclic aromatic cores within the stacks was found to be 3.41 Å. In the triclinic crystalline form of **2a** (Figure 1, right), the molecules arrange in flat layers which are themselves slip-stacked in the perpendicular direction with an interplanar distance of 3.36 Å, a packing pattern which is very similar to graphite (3.37 Å).[20] In both

Table 1. Selected Details of Crystal Structures

compd	crystallization solvent	space group	interplanar distance (Å)
2a	methanol or chloroform	$C2/c$	3.41
2a	pentane/ethyl acetate	$P\bar{1}$	3.36
2b	methanol	$P\bar{1}$	3.48
2c	methanol	$P2_1/n$	3.48/3.50
2c	hexane/ethyl acetate	$P2_1/n$	3.48
3[a]	THF	$C2/c$	3.36
4a	THF	$P\bar{1}$	3.57
4b	chloroform	$P\bar{1}$	3.36
5[a]	toluene	$P2_1/c$	4.53
6	chloroform	$P2_1/n$	3.41

[a]Compound crystallized as a solvate; therefore, solvent molecules are embedded in the solid-state structure.

modifications, weak intermolecular hydrogen bonds are found between the nitrogen and the aromatic hydrogen atoms of the neighboring molecules (2.53–2.58 Å).

A similar type of polymorphism was observed for compound **2c**: single crystals suitable for X-ray diffraction were obtained from methanol and a mixture of hexane and ethyl acetate. In both cases, monoclinic single crystals (space group $P2_1/n$) were found, but with significantly different cell data. In the crystals obtained from hexane/ethyl acetate, the crystal packing pattern displays a herringbone arrangement (Figure 2a) with interplanar distances of 3.48 and 3.50 Å, respectively. On the other hand, in the polymorph obtained from methanol the

dx.doi.org/10.1021/jo300894p | J. Org. Chem. 2012, 77, 6107–6116

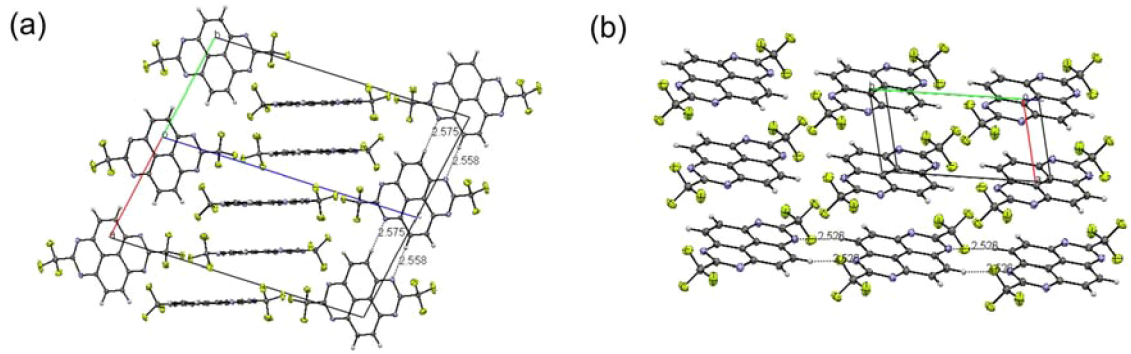

Figure 1. Crystal structures of two polymorphs of compound **2a**: (a) molecular packing in the monoclinic crystals obtained from methanol or chloroform; (b) molecular packing in the triclinic crystals obtained from pentane/ethyl acetate (view along the *b*-axis). Thermal ellipsoids are drawn at the 50% probability level, and weak hydrogen interactions are indicated .

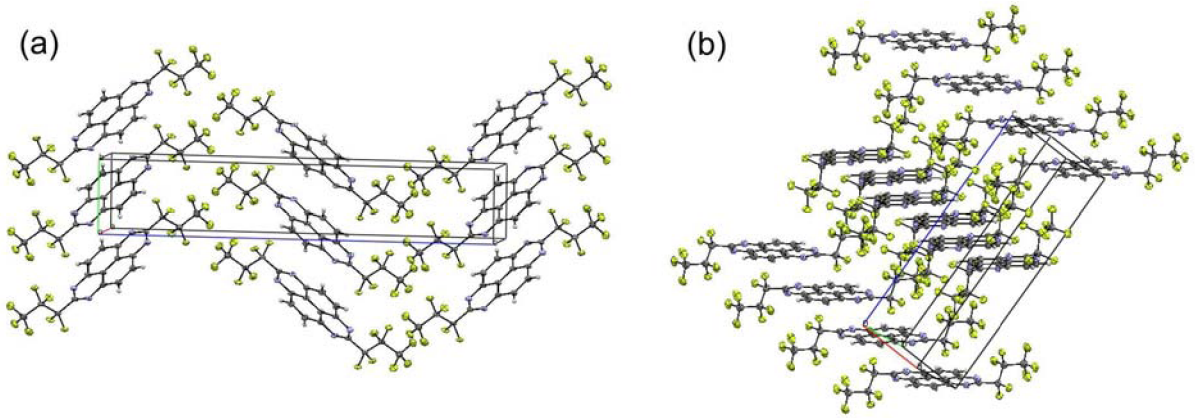

Figure 2. Crystal structures of two polymorphs of compound **2c**: (a) molecular packing in the monoclinic crystals obtained from hexane/ethyl acetate; (b) molecular packing of the polymorph obtained from methanol.

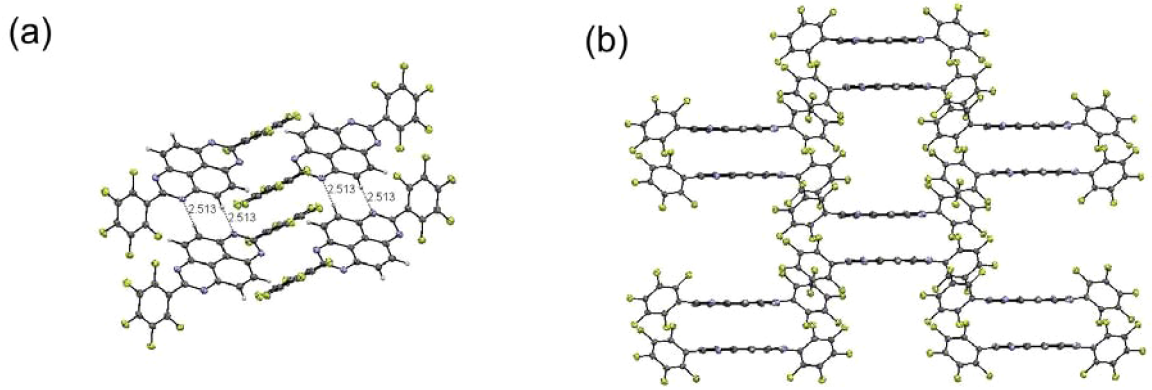

Figure 3. Crystal packing pattern of compound **3**: (a) twisted arrangement of the aryl substituent and weak hydrogen interactions between neighboring molecules within each layer; (b) pairwise arrangement of layers and the $\pi-\pi$ interactions between the perfluorinated phenyl rings in neighboring "sandwich-type layers" (embedded solvent molecules have been omitted for clarity).

molecules are layered with the tetraazapyrene cores essentially being coplanar (Figure 2b). Two types of slipped π-stacks are thus formed ($\pi-\pi$-stacking distance 3.46 Å) with the same lateral orientation of the molecules along the skew stack axis within each stack and the two types of stack rotated by about 90° relative to one another.

The pentafluorophenyl-substituted compound **3** crystallized from THF as a solvate in the form of monoclinic crystals (space group $C2_1/c$). Not surprisingly, the molecular packing pattern observed in this case differs significantly from the ones discussed above (Figure 3a). The structure appears to be dominated by pairwise $\pi-\pi$ interactions between the perfluorinated phenyl rings (interplanar distance 3.56 Å) which are twisted out of the plane of the tetraazapyrene core by 52° in opposite directions.

The pyrene cores of neighboring molecules are thus so strongly shifted with respect to one another that hardly any π-overlap can occur. In this rather open network channels are formed along the crystal *c* axis (Figure 3b), which are filled with

dx.doi.org/10.1021/jo300894p | *J. Org. Chem.* 2012, 77, 6107–6116

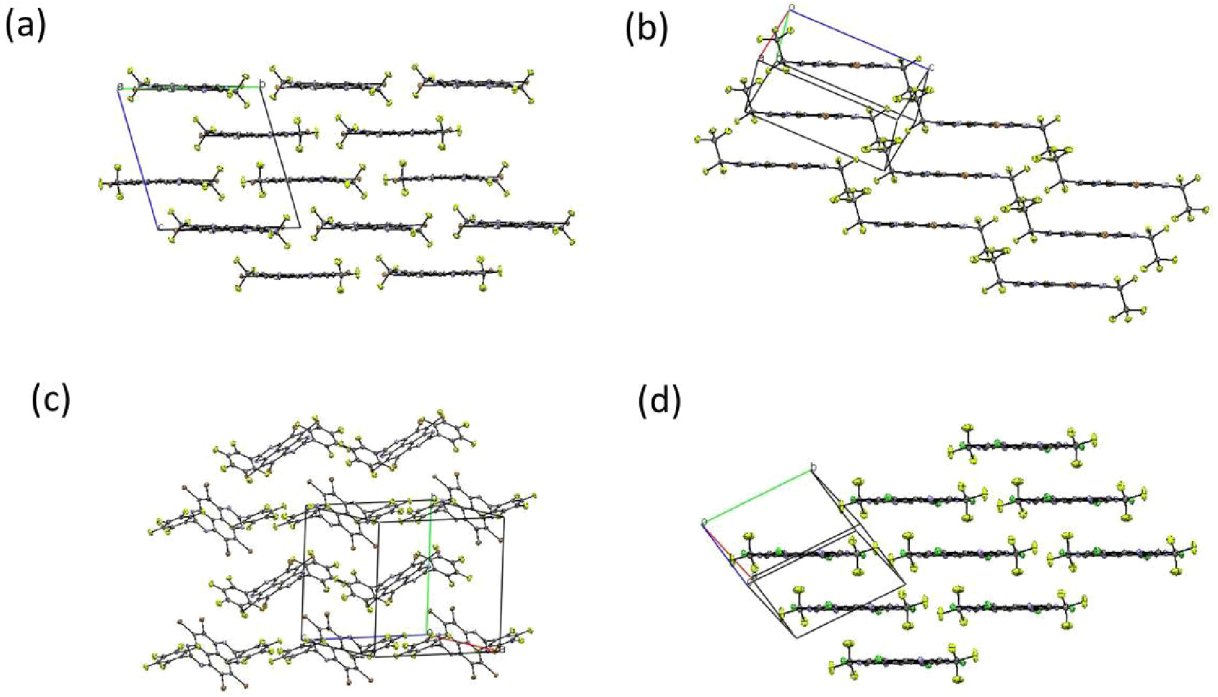

Figure 4. Intermolecular packing patterns of (a) **4a** brickwork arrangement, (b) **4b** ladder-type arrangement, (c) **5** typical herringbone-like structure, and (d) **6** ladder-type arrangement (embedded solvent molecules have been omitted for clarity).

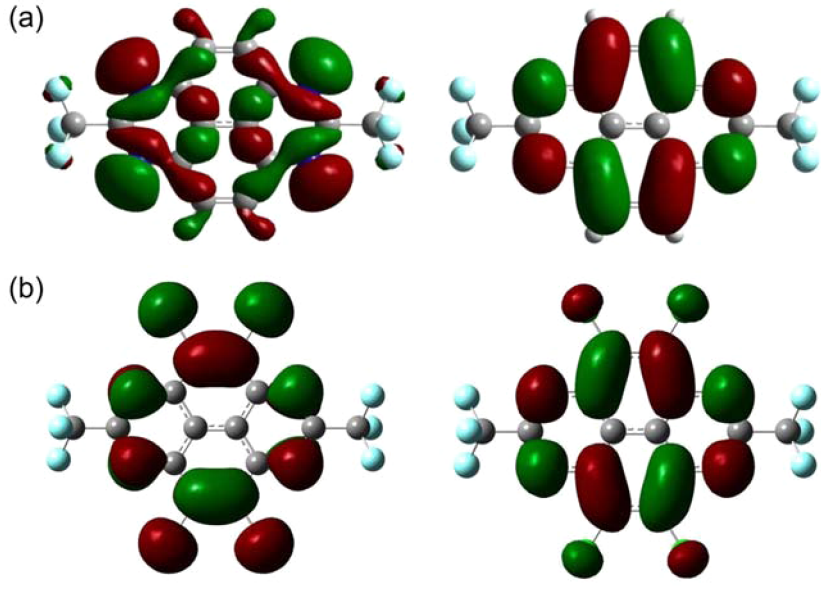

Figure 5. Kohn–Sham HOMO (left) and LUMO (right) of **2a** (a) and its core-chlorinated equivalent **6** (b).

strongly disordered solvent molecules (see the Experimental Section).

In the solid-state structure of the dibrominated tetraazapyrene **4a**, the molecules stack along the *c* axis with an interplanar distance of 3.57 Å (Figure 4a). Within the stacks the molecules are significantly shifted giving rise to a brickwork arrangement which may be classified as a two-dimensional stack. Molecules of **4b** build parallel stacks along the shortest axis with an interplanar distance of 3.36 Å (Figure 4b).

The tetrabromo derivative **5** crystallized as a toluene solvate in the form of monoclinic crystals (space group $P2_1/c$). It displays a typical herringbone-like structure with an enhanced interplanar distance of 4.53 Å (Figure 4c). In this case, the perfluorinated phenyl substituents are even further twisted out of the plane of the aromatic core (dihedral angle 74°) than in the solid-state structure of **3** (52°) and no $\pi-\pi$ interactions between adjacent pyrene molecules can be observed.

Finally, in the crystal structure of the 4-fold core-chlorinated tetraazapyrene **6**, the molecules build parallel stacks along the shortest cell axis with an interplanar distance of 3.41 Å (Figure 4d).

To date, polymorphism has been observed for compounds **2a** and **2c**, but it is very likely that other **TAPy**-derivatives display polymorphism as well. Furthermore, different inter-

dx.doi.org/10.1021/jo300894p | *J. Org. Chem.* 2012, 77, 6107–6116

planar distances ranging from 3.36 to 4.53 Å and very diverging arrangements of the molecules in the solid state, ranging from herringbone structures to brickwork arrangements, have been observed. Apart from the way in which the molecular shapes influence the crystal structures, the conditions of crystallization, in particular the solvent, play an important role. When processing thin organic layers from the liquid phase, this aspect therefore needs to be considered.

Theoretical Modeling and Electrochemistry. The redox properties of organic compounds, which are relevant for potential applications as semiconductors, are primarily determined by their frontier orbital energies.[21] The relative HOMO and LUMO energetic positions of an organic material indicate which type of charge carriers are expected to be predominant and furthermore allow a prediction of the stability of this material in typical organic semiconductors. In the case of organic n-type materials, in which the charge transport occurs predominantly by hopping through the LUMO energy levels, low-lying LUMOs are thought to be required for an efficient electron injection into the semiconductor.[3d,21] Furthermore, the electron affinities (EA) of the organic material should be within the range of 2.8 to 4.0 eV to provide the stability of the radical anion species against ambient oxidants, such as water and oxygen.[21−23] The size of the molecular π-system is one factor that determines the electron affinity: The smaller a π-system is, the less space is available for an injected electron to delocalize along that system, implying that smaller π-systems (as in naphthalene or pyrene derivatives) generally have lower electron affinities than larger π-systems (as in perylenes or oligoacenes).

The electronic structure of the tetraazapyrene derivatives reported in this work were modeled at the B3PW91/6-31 g(d,p) level of DFT which has been validated for this type of systems in previous studies.[4,5] Molecular geometries were optimized and the energy minima verified by frequency analysis. Electron affinities were determined by using a basis set that includes diffuse functions (6-311+g(d,p)). An energy optimization of the corresponding anionic species of each compound was carried out and subtraction of the minimum energy of the neutral form gives the electron affinity.[24]

Bond lengths and angles obtained from the calculations were generally in good agreement with those found in the crystal structure analyses (see Supporting Information). The Kohn−Sham HOMO and LUMO of compound **2a** and **6** displayed in Figure 5 represent the frontier orbitals of the **TAPy** derivatives investigated in this work. The longitudinal axis of the molecule, connecting the carbon atoms at position 2 and 7, lies in a nodal plane of the frontier orbitals. As a consequence, the substituents in these positions only have a small effect on the frontier orbital energies.

Table 2 summarizes the calculated HOMO and LUMO energies and the electron affinities of **TAPy** derivatives **2a−c** and **3** which have no core substituents. Compounds **2a−c** display HOMO energies of about −7.70 eV and LUMO energies of about −3.70 eV. It is not surprising, however, that with increasing length of the perfluorinated alkyl chain the energies are not significantly affected because the substituents at the positions 2 and 7 lie on the nodal plane referred to above. Insertion of pentafluorophenyl substituents to the pyrene core (**3**) also results in lowering of the HOMO and LUMO energy levels compared to the parent compound **II** but the effect is less prominent than for the perfluoroalkyl groups (Table 2). This observation is in accordance with the reactivity of derivatives **2a−c** and **3** in the bromination procedures discussed above.

Table 2. Calculated HOMO and LUMO Energies and EAs and Measured LUMO Energies for the 2,7-Substituted TAPy Derivatives 2a−c and 3 (Compared to the Computed Values of the Parent Compound II)

compd	HOMO[a] (eV)	LUMO DFT[a] (eV)	LUMO CV (eV)	EA[b] (eV)
II	−7.10	−3.11	−3.38	1.92
2a	−7.69	−3.69	−3.75	2.65
2b	−7.72	−3.72	−3.77	2.72
2c	−7.74	−3.73	−3.78	2.77
3	−7.09	−3.40	−3.61	2.55

[a]Determined with B3PW91/6-31 g(d,p). [b]Determined with B3PW91/6-311+g(d,p).

While bromination of **TAPy 3** can still be accomplished with elemental bromine in the presence of a catalyst, the deactivation of the tetraazpyrene which is caused by introduction of the stronger electron-withdrawing perfluoroalkyl substituents is too strong and therefore bromination can only be achieved with the use of DBI. As expected, in the same way as the LUMO energies were lowered the calculated electron affinities of tetraazapyrenes **3** (2.55 eV) and **2a−c** (2.65−2.77 eV) increased (Table 2).

In order to compare the results obtained from theoretical modeling with experimentally accessible data, cyclic voltammograms were recorded for all tetraazapyrenes except for compound **1b**, which was found to be insufficiently soluble in THF. It is well-established that the measured reduction potentials may be correlated with the LUMO energies.[25] All CVs display two reversible reduction half waves that correspond to the sequential formation of the mono- and dianions (Figure 6).

Using ferrocene as an internal standard confirmed that all redox waves corresponded to one-electron reductions and furthermore allowed the estimation of the LUMO energies for all compounds. The cyclic voltammograms of the parent compound **II** (dotted line) and compound **2a** (gray line) displayed in Figure 6 nicely visualize the effect of the electron-

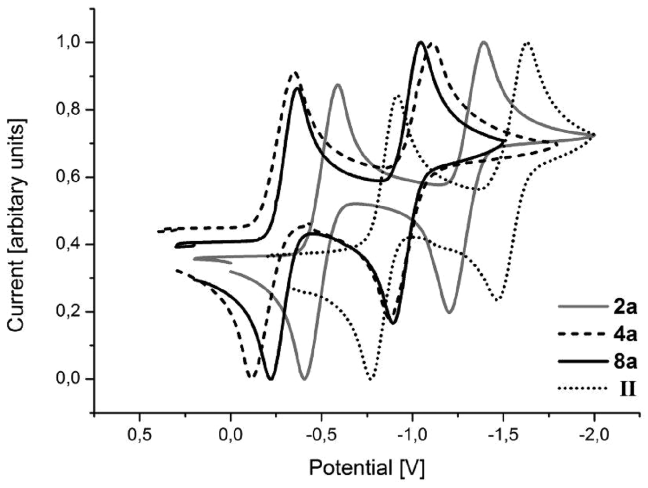

Figure 6. Cyclic voltammograms of the parent compound **II**, the 2,7-disubstituted derivative **2a**, and the core-substituted tetraazapyrenes **4a** and **8a** recorded in THF (sweep rate 50 mV s^{-1}; supporting electrolyte Bu_4NPF_6).

dx.doi.org/10.1021/jo300894p | J. Org. Chem. 2012, 77, 6107−6116

withdrawing trifluoromethyl group by a significant shift of the two reversible redox waves of **2a** to higher potentials.

The LUMO energy levels obtained from the CV data of **2a–c** are slightly lower than the values calculated at the level of DFT. However, for **3**, the difference between theoretically and experimentally determined LUMO energies is greater (0.21 eV), an observation which has been previously made in our group for aryl-substituted polycyclic aromatics.[5] As indicated above, the introduction of substituents at the aromatic core is expected to influence the electronic properties of the **TAPy** derivatives significantly which is evident when comparing the data for the 4-fold core-chlorinated and brominated species **1a** and **1b** to the parent compound **II** (Table 3). The LUMO energies of **1a** and **1b** are decreased by >0.50 eV and the electron affinities of, respectively, 2.56 and 2.60 eV are significantly higher than that of the parent compound **II**.

Table 3. Calculated HOMO and LUMO Energies and EAs and Measured LUMO Energies for the Core-Substituted TAPy Derivatives (Compared to the Values of the Parent Compound II)

compd	HOMO[a] (eV)	LUMO DFT[a] (eV)	LUMO CV (eV)	EA[b] (eV)
II	−7.10	−3.11	−3.38	1.92
1a	−7.49	−3.86	−3.81	2.56
1b	−7.29	−3.62	*c*	2.60
4a	−7.73	−3.96	−4.00	3.01
4b	−7.76	−3.98	−4.00	3.07
4c	−7.76	−3.99	−4.01	3.12
5	−7.23	−3.80	−3.98	3.07
6	−7.90	−4.16	−4.14	3.71
7a	−7.19	−3.85	−3.65	3.09
7b	−6.96	−3.50	−3.57	2.79
8a	−7.44	−4.04	−3.91	3.25
8b	−7.35	−3.84	−3.89	3.09

[a]Determined with B3PW91/6-31 g(d,p). [b]Determined with B3PW91/6-311+g(d,p). [c]Solubility of compound **1b** in THF was not sufficient for a CV measurement.

As a next step, the introduction of bromine and chlorine atoms at the pyrene core combined with perfluorinated alkyl chains in position 2 and 7 was studied (compounds **4a–c**, **5**, and **6**) as well as the properties of the Suzuki cross-coupled products **7a**,**b** and **8a**,**b**. Like the introduction of perfluoroalkyl substituents to the parent compound in positions 2 and 7 (Table 2) the subsequent addition of further electron-withdrawing groups, such as bromine (**4a–c**) or chlorine (**6**), to the pyrene core led to an even further decrease of LUMO energy levels and an increase of electron affinities (Table 3). Also in this case, the cyclic voltammograms of **2a** (gray line) and **4a** (dashed line) displayed in Figure 6 illustrate the effect of core-substitution.

Substitution of the bromine atoms of **1b** and **4a** by *p*-cyanophenyl groups decreases the theoretically determined LUMO level, the effect being significant only for the Suzuki cross-coupled product **7a**. According to the experimentally obtained values on the other hand, the LUMO energy level of **8a** is slightly higher than that of **4a** but still in the same range and the LUMO energy level of **7a** is actually considerably higher than expected (Table 3). However, in both cases the EAs are increased significantly from 2.60 eV (**1b**) to 3.09 eV (**7a**) and 3.01 eV (**4a**) to 3.25 eV (**8a**), respectively. The effect of the *p*-trifluorophenyl substituent on the electronic properties of the **TAPy**s is similar but less prominent (Table 3).

Electron Mobilities in Thin Layers of TAPy Derivatives. The redoxchemical properties of all **TAPy** derivatives suggest that these molecules might have semiconducting properties. To this end, thin-film transistors (TFTs) were fabricated by vapor deposition of the organic material in high vacuum. Source and drain metal contacts were subsequently installed on the organic layer by vacuum deposition through a shadow mask, giving rise to a bottom-gate, top-contact TFT architecture. The TFTs were measured in ambient air with a humidity of about 50% under yellow laboratory light. All tested substances displayed either n-type or no semiconducting properties, while ambipolar or p-type behavior was not observed, confirming the notion that the **TAPy**s presented in this work are potential electron conducting materials.

Neither the 4-fold core-chlorinated and brominated **TAPy** derivatives **1a** and **1b** nor the Suzuki cross-coupling products **7a**,**b** and **8a** displayed a measurable field effect, despite the fact that their calculated LUMO energies and EAs appear favorable for n-channel semiconduction. For the latter, the nonplanar overall molecular geometry due to the bulky phenyl rings may inhibit an effective π-overlap on the device surface. Moreover, AFM studies of vapor deposited films of **1b**, **7b**, and **8a** revealed a very rough, uneven. and amorphous morphology which does not seem to be suited for conduction (see the Supporting Information).

Whereas **TAPy** derivatives **2a–c** proved to be too volatile to be processed by vapor deposition, a small field effect was measured for **TAPys 3**, **4a**,**c**, and **5**. Table 4 provides an overview of all measured electron mobilities which we found to be low compared to the recently studied tetraazaperopyrenes.[6]

Table 4. Electron Mobilities Measured in Bottom-Gate, Top-Contact OTFTs for TAPys 3, 4a,c, and 5

compd	**3**	**4a**	**4c**	**5**
electron mobility ($cm^2/(V\ s)$)	1×10^{-3}	6×10^{-4}	5×10^{-5}	6×10^{-5}

CONCLUSION

In summary, we have developed a general way to synthesize 2,7-disubstituted tetraazapyrenes in good yields. These compounds can be further derivatized by core chlorination and bromination, creating valuable starting materials for subsequent Suzuki cross-coupling reactions. Single crystals suited for X-ray diffraction have been grown from different organic solvents, revealing polymorphism for some compounds. The LUMO energies have been calculated from the reduction potentials obtained by cyclic voltammetry and compared to the ones computed by DFT. LUMO energies of −3.57 to −4.14 eV and electron affinities ranging from 2.55 to 3.71 eV clearly indicate that tetraazapyrenes that bear electron-withdrawing groups are potential n-type semiconductors. Organic TFTs have been fabricated by vacuum deposition and the largest electron mobility of 0.001 $cm^2/(V\ s)$ was found for compound **3**. It is well-known that the right combination of electrochemical properties and crystal packing is required for large electron mobilities As we have shown in this first study, the tetraazapyrenes offer the potential for further derivatization and thus may give access to novel organic semiconductors.

dx.doi.org/10.1021/jo300894p | J. Org. Chem. 2012, 77, 6107–6116

EXPERIMENTAL SECTION

1,4,5,8-Tetraaminonaphthalene hexachlorostannate (**I**)[14] and the parent compound 1,3,6,8-tetraazapyrene (**II**)[7] were prepared according to literature methods.

4,5,9,10-Tetrachloro-1,3,6,8-tetraazapyrene (1a). A 420 mg (2.0 mmol) portion of 1,3,6,8-tetraazapyrene (**II**) was dissolved in 50 mL of chlorosulfonic acid, and 86 mg of iodine was added. The mixture was heated to 80 °C, and for a period of 3 h, chlorine gas was passed through the solution. The resulting mixture was allowed to cool to room temperature and stirred for 12 h. It was then poured on ice, and the precipitate was collected by filtration and extracted with toluene. The solvent was removed under reduced pressure to yield 530 mg (1.56 mmol, 78%) of **1a** as a golden-brown solid: mp dec above 250 °C; ^{1}H NMR (399.89 MHz, $CDCl_3$) δ = 10.23 (s, 2H, CH); ^{13}C NMR (150.90 MHz, $CDCl_3$) δ = 158.7 (C^7H), 150.2 ($C^{1/4}$), 140.1 ($C^{2/3}$), 112.0 ($C^{5/6}$); HRMS (EI$^+$) m/z calcd for $C_{12}H_2Cl_4N_4$ 341.9034, found 341.9024. Anal. Calcd for $C_{12}H_2Cl_4N_4$: C, 41.90; H, 0.59; N, 16.29. Found: C, 42.21; H, 0.87; N, 15.87.

4,5,9,10-Tetrabromo-1,3,6,8-tetraazapyrene (1b). A 420 mg (2.0 mmol) portion of 1,3,6,8-tetraazapyrene (**II**) was dissolved in 50 mL of concentrated sulfuric acid, and 86 mg of iodine and 1 mL of bromine (19.5 mmol) were added. The mixture was heated to 80 °C for 3 h and then allowed to cool to room temperature overnight. The reaction mixture was poured on ice, and the precipitate was collected by filtration, washed thoroughly with sodium hydroxide solution, water, methanol, and pentane, and dried in vacuo to yield 920 mg (1.76 mmol, 87%) of **1b** as a light brown solid: mp decomposition above 260 °C; ^{1}H NMR (600.13 MHz, $CDCl_3$) δ = 10.18 (s, 2H, CH); ^{13}C NMR (150.90 MHz, $CDCl_3$) δ = 158.9 (C^7H), 151.6 ($C^{1/4}$), 136.7 ($C^{2/3}$), 113.0 ($C^{5/6}$); HRMS (EI$^+$) m/z calcd for $C_{12}H_2{}^{79}Br_2{}^{81}Br_2N_4$ 521.6972, found 521.6960. Anal. Calcd for $C_{12}H_2Br_4N_4$: C, 27.62; H, 0.39; N, 10.74. Found: C, 27.82; H, 0.35; N, 10.67.

General Procedure for the Preparation of 2,7-Disubstituted Tetraazapyrene Derivatives. To a suspension of 1.0 g (1.9 mmol) of 1,4,5,8-tetraaminonaphthalene hexachlorostannate (**I**) in 30 mL of abs THF was added 0.5 mL of abs triethylamine under argon. The corresponding anhydride (7.9 mmol) was added slowly under ice cooling. The reaction mixture was heated under reflux for 72 h, and then it was allowed to cool to room temperature. The solvent was removed under vacuum, and the residue was purified by column chromatography (silica, *n*-hexane/ethyl acetate 4:1). The product was recrystallized from methanol three times.

2,7-Bis(trifluoromethyl)-1,3,6,8-tetraazapyrene (2a). Anhydride: trifluoroacetic anhydride; yield 407 mg (1.19 mmol, 62%) of **2a** as a beige solid; mp 179 °C; ^{1}H NMR (600.13 MHz, $CDCl_3$) δ = 8.92 (s, 4H, CH); ^{13}C NMR (150.92 MHz, $CDCl_3$) δ = 156.1 (q, $^2J_{CF}$ = 37.3 Hz, C^7), 153.7 ($C^{1/4}$), 137.4 ($C^{2/3}$), 120.0 (q, $^1J_{CF}$ = 277.0 Hz, CF_3), 114.0 ($C^{5/6}$); ^{19}F NMR (376.27 MHz, $CDCl_3$) δ = −68.64 (s, CF_3); HRMS (EI$^+$) m/z calcd for $C_{14}H_4F_6N_4$ 342.0340, found 342.0352. Anal. Calcd for $C_{14}H_4F_6N_4$: C, 49.14; H, 1.18; N, 16.37. Found: C, 49.09; H, 1.35; N, 16.43.

2,7-Bis(pentafluoroethyl)-1,3,6,8-tetraazapyrene (2b). Anhydride: pentafluoropropionic anhydride; yield 290 mg (0.66 mmol, 45%) of **2b** as a beige solid; mp 183 °C; ^{1}H NMR (399.89 MHz, $CDCl_3$,) δ = 8.90 (s, 4 H, CH); ^{13}C NMR (150.90 MHz, $CDCl_3$) δ = 156.3 (t, $^2J_{CF}$ = 25.5 Hz, C^7), 153.6 ($C^{1/4}$), 137.4 ($C^{2/3}$), 128.9 (tq, $^1J_{CF}$ = 285.3 Hz, $^2J_{CF}$ = 36.0 Hz, CF_3), 113.8 ($C^{5/6}$), 110.2 (qt, $^1J_{CF}$ = 258.3 Hz, $^2J_{CF}$ = 36.0 Hz, CF_2); ^{19}F NMR (79 MHz, $CDCl_3$,) δ = −81.7 (t, 6F, $^3J_{FF}$ = 1.8 Hz, CF_3), 115.5 (q, 4F, $^3J_{FF}$ = 1.8 Hz, CF_2); HRMS (EI$^+$) m/z calcd for $C_{16}H_4F_{10}N_4$ 442.0276, found 442.0270. Anal. Calcd for $C_{16}H_4F_{10}N_4$: C, 43.46; H, 0.91; N, 12.67. Found: C, 43.67; H, 1.15; N, 12.66.

2,7-Bis(heptafluoropropyl)-1,3,6,8-tetraazapyrene (2c). Anhydride: heptafluorobutyric anhydride: yield 280 mg (0.52 mmol, 36%) of **2c** as a beige solid; mp 185 °C; ^{1}H NMR (399.98 MHz, $CDCl_3$) δ = 8.94 (s, 4H, CH). ^{13}C NMR (150.90 MHz, $CDCl_3$) δ = 156.4 (t, $^2J_{CF}$ = 25.8 Hz, C^7), 153.6 ($C^{1/4}$), 137.4 ($C^{2/3}$), 119.1 − 107.8 (m, C_3F_7), 113.8 ($C^{5/6}$); ^{19}F NMR (376.27 MHz, $CDCl_3$) δ = −80.1 (t, 6F, $^3J_{FF}$ = 9.2 Hz, CF_3), −113.7 (q, 4F, $^3J_{FF}$ = 9.1 Hz, CF_2), −125.4 (s, 4F, CF_2); HRMS (EI$^+$) m/z calcd for $C_{18}H_4F_{14}N_4$ 542.0212, found 542.0231. Anal. Calcd for $C_{18}H_4F_{14}N_4$: C, 39.87; H, 0.74; N, 10.33. Found: C, 39.88; H, 1.04; N, 10.54.

2,7-Bis(pentafluorophenyl)-1,3,6,8-tetraazapyrene (3). Anhydride: pentafluorophenyl anhydride: yield 457 mg (0.85 mmol, 44%) of **3** as a beige solid; mp 255 °C; ^{1}H NMR (399.98 MHz, $CDCl_3$) δ = 8.80 (s, 4H, CH). ^{13}C NMR (150.90 MHz, $CDCl_3$) δ = 156.7 (C^7), 153.5 ($C^{1/4}$), 146.2 (C^{Phenyl}-F), 144.6 (C^{Phenyl}-F), 138.7 (C^{Phenyl}-F), 136.9 ($C^{2/3}$), 115.2 (C^{Phenyl}-C^7), 112.7 ($C^{5/6}$); ^{19}F-NMR (79 MHz, $CDCl_3$) δ = −160.8 (m, 4F), −151.4 (m, 2F), −141.9 (m, 4F); HRMS (EI$^+$) m/z calcd for $C_{24}H_4F_{10}N_4$ 538.0276, found 538.0260.

General Procedure for the Preparation of 4,9-Dibrominated 2,7-Perfluoroalkylated Tetraazapyrene Derivatives. 2,7-Bis-(perfluoroalkyl)-1,3,6,8-tetraazapyrene (0.5 mmol) was dissolved in 30 mL of concentrated sulfuric acid. Dibromoisocyanuric acid (574 mg, 2.0 mmol) was added, and the resulting reaction mixture was stirred under the exclusion of light for 48 h at room temperature. An additional amount of 574 mg (2.0 mmol) of dibromoisocyanuric acid was added, and the mixture was stirred under the exclusion of light for 12 h at room temperature. Then it was poured on ice, neutralized with sodium hydroxide, and extracted with methylene chloride. The organic phase was washed with water and brine and dried over sodium sulfate. The solvent was evaporated in vacuo, and the solid residue was recrystallized from methanol twice.

2,7-Bis(trifluoromethyl)-4,9-dibromo-1,3,6,8-tetraazapyrene (4a): starting compound **2a**; yield 50 mg (0.1 mmol, 20%) of **4a** as a beige solid; mp 323 °C; ^{1}H NMR (600.13 MHz, $CDCl_3$) δ = 9.26 (s, 2H, CH); ^{13}C NMR (150.90 MHz, $CDCl_3$) δ = 156.8 (q, $^2J_{CF}$ = 37.8 Hz, C^7), 154.1 (C^4), 152.0 (C^1) 139.4 (C^3), 135.1 (C^2), 119.7 (q, $^1J_{CF}$ = 276.3 Hz, CF_3), 113.5 ($C^{5/6}$); ^{19}F NMR (79 MHz, $CDCl_3$) δ = −68.67 (s, 6F, CF_3); HRMS (EI$^+$) m/z calcd for $C_{14}H_2Br_2F_6N_4$ 497.8550, found 497.8555. Anal. Calcd for $C_{14}H_2Br_2F_6N_4$: C, 33.63; H, 0.40; N, 11.21. Found: C, 33.49; H, 0.53; N, 11.05.

2,7-Bis(pentafluoroethyl)-4,9-dibromo-1,3,6,8-tetraazapyrene (4b): starting compound **2b**; yield 51 mg (0.09 mmol, 17%) of **4b** as a beige solid; mp 303 °C; ^{1}H NMR (600.13 MHz, $CDCl_3$) δ = 9.28 (s, 2H, CH); ^{13}C NMR (150.90 MHz, $CDCl_3$) δ = 157.1 (t, $^2J_{CF}$ = 26.1 Hz, C^7), 154.1 (C^4), 151.9 (C^1) 139.4 (C^3), 135.1 (C^2), 118.8 (tq, $^1J_{CF}$ = 287.0 Hz, $^2J_{CF}$ = 36.1 Hz, CF_3), 113.4 ($C^{5/6}$), 109.9 (qt, $^1J_{CF}$ = 256.6 Hz, $^2J_{CF}$ = 37.0 Hz, CF_2); ^{19}F NMR (79 MHz, $CDCl_3$) δ = −81.56 (m, 6F, CF_3), −115.24 (m, 4F, CF_2); HRMS (EI$^+$) m/z calcd for $C_{16}H_2Br_2F_{10}N_4$ 597.8487, found 597.8489.

2,7-Bis(heptafluoropropyl)-4,9-dibromo-1,3,6,8-tetraazapyrene (4c): starting compound **2c**; yield 56 mg (0.08 mmol, 16%) of **4c** as a beige solid; mp 330 °C; ^{1}H NMR (600.13 MHz, $CDCl_3$) δ = 9.29 (s, 2H, CH); ^{13}C NMR (150.90 MHz, $CDCl_3$) δ = 157.1 (t, $^2J_{CF}$ = 26.0 Hz, C^7), 154.0 (C^4), 151.9 (C^1) 139.4 (C^3), 135.2 (C^2), 117.8 (tq, 6F, $^1J_{CF}$ = 288.5 Hz, $^2J_{CF}$ = 33.5 Hz, CF_3), 113.4 ($C^{5/6}$), 111.5 (tt, 4F, $^1J_{CF}$ = 259.8 Hz, $^2J_{CF}$ = 30.6 Hz, CF_2), 109.8 (m, 4F, CF_2); ^{19}F NMR (79 MHz, $CDCl_3$) δ = −80.03 (t, 6F, $^3J_{FF}$ = 8.9 Hz, CF_3), −113.57 (m, 4F, CF_2), −125.34 (m, 4F, CF_2); HRMS (EI$^+$) m/z calcd for $C_{18}H_2Br_2F_{14}N_4$ 697.8423, found 697.8399. Anal. Calcd for $C_{18}H_2Br_2F_{14}N_4$: C, 30.88; H, 0.29; N, 8.00. Found: C, 30.53; H, 0.65; N, 7.86.

2,7-Bis(pentafluorophenyl)-4,5,9,10-tetrabromo-1,3,6,8-tetraazapyrene (5). 2,7-Bis(pentafluorophenyl)-1,3,6,8-tetraazapyrene **3** (100 mg, 0.19 mmol) was dissolved in 50 mL of concentrated sulfuric acid, and 86 mg of iodine and 1.6 mL of bromine (31.2 mmol) were added. The mixture was heated to 80 °C for 3 h and then allowed to cool to room temperature overnight. The reaction mixture was poured on ice, and the precipitate was collected by filtration, washed thoroughly with sodium hydroxide solution, water, methanol, and pentane, and dried in vacuo to yield 29 mg (0.03 mmol, 18%) of **5** as a light brown solid: mp 326 °C; ^{13}C NMR (150.90 MHz, $CDCl_3$) δ = 158.2 (C^7), 152.5 ($C^{1/4}$), 137.2 ($C^{2/3}$), 111.3 ($C^{5/6}$), perfluorinated aryl carbon signals were not observed; ^{19}F NMR (79 MHz, $CDCl_3$) δ = −160.8 (m, 4F), −151.4 (m, 2F), −141.9 (m, 4F); HRMS (EI$^+$) m/z calcd for $C_{24}Br_4F_{10}N_4$ 849.6697, found 849.6684.

dx.doi.org/10.1021/jo300894p | J. Org. Chem. 2012, 77, 6107−6116

2,7-Bis(trifluoromethyl)-4,5,9,10-tetrachloro-1,3,6,8-tetraazapyrene (6). 2,7-Bis(trifluoromethyl)-1,3,6,8-tetraazapyrene **2a** (50 mg, 0.15 mmol) was dissolved in 10 mL of concentrated sulfuric acid. Dichloroisocyanuric acid (300 mg, 1.5 mmol) was added, and the resulting reaction mixture was stirred under the exclusion of light for 10 days at 100 °C. Then it was poured on ice, neutralized with sodium hydroxide, and extracted with methylene chloride. The organic phase was washed with water and brine and dried over sodium sulfate. The solvent was evaporated in vacuo, and the solid residue was recrystallized three times from methanol and three times from THF to yield 10 mg (0.02 mmol, 13%) of **6** in the form of colorless crystals: ^{13}C NMR (150.90 MHz, $CDCl_3$) δ = 157.0 (q, $^2J_{CF}$ = 38.7 Hz, C^7), 151.6 (C^1), 141.5 ($C^{2/3}$), 119.5 (q, $^1J_{CF}$ = 275.6 Hz, CF_3), 111.8 ($C^{5/6}$); ^{19}F NMR (376.27 MHz, $CDCl_3$) δ = −68.62 (s, 6F, CF_3); HRMS (EI$^+$) m/z calcd for $C_{14}Cl_4F_6N_4$ 477.8781, found 477.8803.

General Procedure for Suzuki Cross-Coupling Reactions. An oven-dried Schlenk tube was loaded with 1 equiv of brominated tetraazapyrene **1a** or **4a**, 4−8 equiv of the corresponding boronic acid, 6−10 equiv of cesium carbonate, and 0.1−0.2 equiv of Pd(dppf)Cl_2 and evacuated and refilled with argon three times. Absolute 1,4-dioxane (30 mL) was added, the Schlenk tube was sealed with a glass cap, and the reaction mixture was stirred at 100 °C for 48 h. The mixture was allowed to cool to room temperature, the solvent was evaporated, and the solid residue was extracted with chloroform. The organic phase was washed with water and brine, dried over sodium sulfate, and evaporated in vacuo.

4,5,9,10-Tetrakis(4-cyanophenyl)-1,3,6,8-tetraazapyrene (7a): starting compounds 120 mg (0.23 mmol) of 4,5,9,10-tetrabromo-1,3,6,8-tetraazapyrene (**1b**) and 270 mg (1.84 mmol) of 4-cyanophenylboronic acid; yield 65 mg (0.12 mmol, 46%) of **7a** as a light brown solid; mp 458 °C; ^{1}H NMR (600.13 MHz, $CDCl_3$) δ = 10.00 (s, 2H, C^7H), 7.72 (d, 8H, $^3J_{HH}$ = 7.2 Hz), 7.47 (d, 8H, $^3J_{HH}$ = 8.4 Hz); ^{13}C NMR (150.90 MHz, $CDCl_3$) δ = 158.0 (C^7), 151.6 ($C^{1/4}$), 144.9 ($C^{2/3}$), 139.1 (C^8), 132.0 (C^9), 131.8 (C^{10}), 118.2 (CN), 114.0 ($C^{5/6}$), 112.7 (C^{11}); HRMS (FAB$^+$) m/z calcd for $C_{40}H_{19}N_8$ 611.1732, found 611.1752.

4,5,9,10-Tetrakis(4-trifluoromethylphenyl)-1,3,6,8-tetraazapyrene (7b): starting compounds 150 mg (0.29 mmol) of 4,5,9,10-tetrabromo-1,3,6,8-tetraazapyrene (**1b**) and 441 mg (2.32 mmol) of 4-trifluoromethylphenylboronic acid yield 45 mg (0.7 mmol, 24%) of **7b** as a beige solid; mp 395 °C; ^{1}H NMR (600.13 MHz, $CDCl_3$) δ = 10.04 (s, 2H, C^7H), 7.67 (d, 8H, $^3J_{HH}$ = 8.2 Hz), 7.49 (d, 8H, $^3J_{HH}$ = 8.0 Hz); ^{13}C NMR (150.90 MHz, $CDCl_3$) δ = 157.9 (C^7), 151.9 ($C^{1/4}$), 145.3 ($C^{2/3}$), 138.4 (C^8), 131.8 (C^9), 130.2 (C^{11}), 125.0 (C^{10}), 123.0 (CF_3), 113.9 ($C^{5/6}$); ^{19}F NMR (79 MHz, $CDCl_3$) δ = −62.68 (s, 12F, CF_3); HRMS (EI$^+$) m/z calcd for $C_{40}H_{18}F_{12}N_4$ 782.1340, found 782.1329.

2,7-Bis(trifluoromethyl)-4,9-bis(4-cyanophenyl)-1,3,6,8-tetraazapyrene (8a): starting compounds 100 mg (0.20 mmol) of 2,7-bis-(trifluoromethyl)-4,9-dibromo-1,3,6,8-tetraazapyrene (**4a**) and 118 mg (0.80 mmol) of 4-cyanophenylboronic acid: yield 65 mg (0.12 mmol, 60%) of **8a** as a light gray solid; mp 420 °C; ^{1}H NMR (600.13 MHz, $CDCl_3$) δ = 9.02 (s, 2H, C^3H), 8.14 (d, 4H, $^3J_{HH}$ = 8.1 Hz), 7.98 (d, 4H, $^3J_{HH}$ = 8.2 Hz); ^{13}C NMR (150.90 MHz, $CDCl_3$) δ = 156.2 (C^7), 153.7 (C^4), 151.9 (C^1), 147.1 (C^2), 138.7 (C^8), 136.4 (C^3), 132.5 (C^{10}), 131.5 (C^9), 118.2 (CN), 114.3 ($C^{5/6}$), 114.0 (C^{11}); ^{19}F NMR (79 MHz, $CDCl_3$) δ = −68.76 (s, 6F, CF_3); HRMS (MALDI$^+$) m/z calcd for $C_{28}H_9F_6N_6$ 543.0787, found 543.0767.

2,7-Bis(trifluoromethyl)-4,9-bis(4-trifluoromethylphenyl)-1,3,6,8-tetraazapyrene (8b): starting compounds 130 mg (0.26 mmol) of 2,7-bis(trifluoromethyl)-4,9-dibromo-1,3,6,8-tetraazapyrene (**4a**) and 197 mg (1.04 mmol) of 4-trifluoromethylphenylboronic acid; yield 35 mg (0.06 mmol, 23%) of **8b** as a white solid; mp 419 °C; ^{1}H NMR (600.13 MHz, $CDCl_3$) δ = 9.02 (s, 2H, C^3H), 8.20 (d, 4H, $^3J_{HH}$ = 8.0 Hz), 7.95 (d, 4H, $^3J_{HH}$ = 8.1 Hz); ^{13}C NMR (150.90 MHz, $CDCl_3$) δ = 156.1 (q, $^2J_{CF}$ = 37.2 Hz, C^7), 153.8 (C^4), 152.3 (C^1), 147.7 (C^2), 137.9 (C^8), 136.2 (C^3), 132.1 (q, $^2J_{CF}$ = 33.0 Hz, C^{11}), 131.3 (C^9), 125.8 (C^{10}), 124.8 ($C^{12}F_3$), 119.0 (CF_3), 114.2 ($C^{5/6}$); ^{19}F NMR (79 MHz, $CDCl_3$) δ = −68.76 (s, 6F, CF_3), −62.72 (s, 6F, $C^{12}F_3$); HRMS (MALDI$^+$) m/z calcd for $C_{28}H_9F_{12}N_4$ 629.0630, found 629.0610.

X-ray Crystal Structure Determinations. Crystal data and details of the structure determinations are given in the Supporting Information. Full shells of intensity data were collected at low temperature (T = 100 K, Mo Kα radiation, sealed tube, graphite monochromator, all compounds except **3·thf** or Cu Kα radiation, microfocus tube, multilayer mirror optics for **3·thf**). Data were corrected for air and detector absorption, Lorentz and polarization effects;[26,27] absorption by the crystal was treated numerically (second monoclinic form of **2c** and compound **4b**) or with a semiempirical multiscan method (all others).[27−29]

The structures were solved by direct methods with dual-space recycling (compounds **2a**[30] and **2c**[31,32]) by the heavy atom method combined with structure expansion by direct methods applied to difference structure factors[33] (compound **4b**) or by the charge flip procedure[34] (all others) and refined by full-matrix least-squares methods based on F^2 against all unique reflections.[32,35] All non-hydrogen atoms were given anisotropic displacement parameters. Hydrogen atoms were generally placed at calculated positions and refined with a riding model. When justified by the quality of the data the positions of the hydrogen atoms were taken from difference Fourier syntheses and refined. Due to severe disorder and fractional occupancy, electron density attributed to solvent of crystallization (thf) was removed from the structure (and the corresponding F_{obs}) of **3** with the BYPASS procedure,[36] as implemented in PLATON (SQUEEZE).[37] Crystals of **5** were twinned; after detwinning (approximately twin fractions 0.87:0.13) refinement was carried out against all observations involving domain 1.

Fabrication of the Organic Thin-Film Transistors (TFTs). The TFTs were fabricated in the bottom-gate, top-contact architecture on doped silicon substrates. As the gate electrode, a 20-nm-thick layer of aluminum was deposited by vacuum evaporation directly onto the silicon substrate. The gate dielectric is a combination of 3.6 nm thick AlO_x (grown by plasma oxidation) and a 1.7 nm thick self-assembled monolayer (SAM) of n-tetradecylphosphonic acid (prepared by immersing the substrate with the freshly oxidized aluminum gate electrodes into a 2-propanol solution of n-tetradecylphosphonic acid). A 30 nm thick layer of the corresponding **TAPy** derivative was then vacuum-deposited onto the AlO_x/SAM gate dielectric, and Au source/drain contacts were deposited on top of the semiconductor by vacuum evaporation through a shadow mask. The TFTs have a channel length of 50 μm and a channel width of 1000 μm. Electrical measurements were carried out in air, and field-effect mobilities were extracted from the transfer characteristics in the saturation regime.[6]

■ ASSOCIATED CONTENT

Ⓢ Supporting Information

General experimental methods, compound characterization by ^{1}H and ^{13}C NMR spectra for all compounds and computational and X-ray crystallographic data. This material is available free of charge via the Internet at http://pubs.acs.org.

■ AUTHOR INFORMATION

Corresponding Author

*E-mail: lutz.gade@uni-hd.de.

Present Address

[§]Department of Physics, University of Basel, Klingelbergstrasse 82, CH-4056 Basel, Switzerland

Notes

The authors declare no competing financial interest.

■ ACKNOWLEDGMENTS

We thank the German Ministry of Education and Research (BMBF) for funding of this work within the project POLYTOS

(FKZ: 13N10205) in the Research Network "Forum Organic Electronics".

REFERENCES

(1) (a) Harvey, R. G. *Polycyclic Aromatic Hydrocarbons*; Wiley-VCH: New York, 1997; (b) Topics in Current Chemistry, Vol. *196*: *Carbon Rich Compounds I*; de Meijere, A., Ed.; Springer: Berlin, 1998. (c) Topics in Current Chemistry, Vol. *201*: *Carbon Rich Compounds II: Macrocyclic Oligoacetylenes and Other Linearly Conjugated Systems*; de Meijere, A., Ed.; Springer: Berlin, 1999. (d) Fetzer, J. C. *Large (C ≥ 24) Polycyclic Hydrocarbons: Chemistry and Analysis*; John Wiley and Sons: New York, 2000.

(2) For recent reviews, see: (a) Würthner, F.; Schmidt, R. *ChemPhysChem* **2006**, *7*, 793−797. (b) Anthony, J. E. *Chem. Rev.* **2006**, *106*, 5028−5048. (c) *Organic Electronics*; Klauk, H., Ed.; Wiley-VCH: Weinheim, Germany, 2006. (d) *Organic Field-Effect Transistors*; Bao, Z., Locklin, J., Eds.; Taylor and Francis: Boca Raton, FL, 2007. (e) Wu, J.; Pisula, W.; Müllen, K. *Chem. Rev.* **2007**, *107*, 718−747. (f) Coropceanu, V.; Cornil, J.; da Silva Filho, D. A.; Olivier, Y.; Silbey, R.; Brédas, J.-L. *Chem. Rev.* **2007**, *107*, 926−952. (g) Shirota, Y.; Kageyama, H. *Chem. Rev.* **2007**, *107*, 953−1010. (h) Katz, H. E.; Huang, J. *Annu. Rev. Mater. Res.* **2009**, *39*, 71−92. (i) Pisula, W.; Mishra, A. K.; Li, J.; Baumgarten, M.; Müllen, K. Carbazole-based Conjugated Polymers as Donor Material for Photovoltaic Devices. In *Organic Photovoltaics: Materials, Device Physics and Manufacturing Technologies*; Brabec, C., Dyakonov, V., Scherf, U., Eds.; Wiley-VCH: Weinheim, 2008; pp 93−128. (j) Thompson, B. C.; Fréchet, J. M. J.. *Angew. Chem., Int. Ed.* **2008**, *47*, 58−77. (k) Anthony, J. E. *Angew. Chem., Int. Ed.* **2008**, *47*, 452−483. (l) Wang, C.; Dong, H.; Hu, W.; Liu, Y.; Zhu, D. *Chem. Rev.* **2012**, *112*, 2208−2267.

(3) See, for example: (a) Jonkheijm, P.; Stutzmann, N.; Chen, Z.; de Leeuw, D. M.; Meijer, E. W.; Schenning, A. P. H. J.; Würthner, F. *J. Am. Chem. Soc.* **2006**, *128*, 9535−9540. (b) Chen, H. Z.; Ling, M. M.; Mo, X.; Shi, M. M.; Wang, M.; Bao, Z. *Chem. Mater.* **2007**, *19*, 816−824. (c) Schmidt, R.; Ling, M. M.; Oh, J. H.; Winkler, M.; Könemann, M.; Bao, Z.; Würthner, F. *Adv. Mater.* **2007**, *19*, 3692−3695. (d) Schmidt, R.; Oh, J. H.; Sun, Y.-S.; Deppisch, M.; Krause, A.-M.; Radacki, K.; Braunschweig, H.; Könemann, M.; Erk, P.; Bao, Z.; Würthner, F. *J. Am. Chem. Soc.* **2009**, *131*, 6215−6228. (e) Qian, H.; Yue, W.; Zhen, Y.; Di Motta, S.; Di Donato, E.; Negri, F.; Qu, J.; Xu, W.; Zhu, D.; Wang, Z. *J. Org. Chem.* **2009**, *74*, 6275−6282. (f) Zhan, X.; Facchetti, A.; Barlow, S.; Marks, T. J.; Ratner, M. A.; Wasielewski, M. R.; Marder, S. R. *Adv. Mater.* **2011**, *23*, 268−284. (g) Hesse, H. C.; Weickert, J.; Hundschell, C.; Feng, X.; Müllen, K.; Nickel, B.; Mozer, A. J.; Schmidt-Mende, L. *Adv. Energy Mater.* **2011**, *1*, 861−869.

(4) Riehm, T.; De Paoli, G.; Konradsson, A. E.; De Cola, L.; Wadepohl, H.; Gade, L. H. *Chem.—Eur. J.* **2007**, *13*, 7317−7329.

(5) (a) Martens, S. C.; Riehm, T.; Geib, S.; Wadepohl, H.; Gade, L. H. *J. Org. Chem.* **2011**, *76*, 609−617. (b) Matena, M.; Riehm, T.; Stöhr, M.; Jung, T. A.; Gade, L. H *Angew. Chem., Int. Ed.* **2008**, *47*, 2414−2417. (c) Matena, M.; Stöhr, M.; Riehm, T.; Björk, J.; Martens, S.; Dyer, M. S.; Persson, M.; Llobo-Checa, J.; Müller, K.; Enache, M.; Wadepohl, H.; Zegenhagen, J.; Jung, T. A.; Gade, L. H. *Chem.—Eur. J.* **2010**, *16*, 2079−2091.

(6) Martens, S. C.; Zschieschang, U.; Wadepohl, H.; Klauk, H.; Gade, L. H. *Chem.—Eur. J.* **2012**, *18*, 3498−3509.

(7) Dimroth, O.; Roos, H. *Liebigs Ann. Chem.* **1927**, *456*, 177−192.

(8) Gerson, F. *Helv. Chim. Acta* **1964**, *47*, 1484−1496.

(9) Dawans, F.; Reichel, B.; Marvel, C. S. *J. Polym. Sci. Part A* **1964**, *2*, 5005−5016.

(10) (a) Plümpe, H.; Bock, M. Ger. Pat. (Bayer AG) DE 1265754, 1964. (b) Plümpe, H.; Bock, M. Ger. Pat. (Bayer AG) DE 1263775, 1964. (c) Plümpe, H.; Bock, M. Bel. Pat. (Bayer AG) BE 659016, 1965.

(11) Pozharskii, A. F.; Koroleva, V. N.; Komissarov, I. V.; Filippov, I. T.; Borovlev, I. V. *Khim.—Farm. Zh.* **1976**, *10*, 34−38.

(12) Aksenov, A. V.; Lyakhovnenko, A. S.; Karaivanov, N. Ts.; Aksenova, I. V. *Chem. Heterocycl. Compd.* **2010**, *46*, 1146−1147.

(13) (a) Ward, E. R.; Johnson, C. D.; Day, L. A. *J. Chem. Soc.* **1959**, 487−493. (b) Vitske, V.; König, C.; Hübner, O.; Kaifer, E.; Himmel, H.-J. *Eur. J. Inorg. Chem.* **2010**, 115−126.

(14) Will, W. *Chem. Ber.* **1895**, *28*, 2234−2235.

(15) (a) Gotthardi, W. *Monatsh. Chem.* **1968**, *99*, 815. (b) Becker, H. G. O. *Organikum*; Wiley-VCH: Weinheim, 2001.

(16) Rosevear, J.; Wilshire, J. F. K. *Aust. J. Chem.* **1980**, *33*, 843−852.

(17) (a) Miyaura, N.; Suzuki, A. *Chem. Rev.* **1995**, *95*, 2457−2483. (b) Alberico, D.; Scott, M. E.; Lautens, M. *Chem. Rev.* **2007**, *107*, 174−238.

(18) Gsänger, M.; Oh, J. H.; Könemann, M.; Höffken, H. W.; Krause, A.-M.; Bao, Z.; Würthner, F. *Angew. Chem., Int. Ed.* **2010**, *49*, 740−743.

(19) Wang, C.; Dong, H.; Li, H.; Zhao, H.; Meng, Q.; Hu, W. *Cryst. Growth Des.* **2010**, *10*, 4155−4160.

(20) Forrest, S. R.; Kaplan, M. L.; Schmidt, P. H. *J. Appl. Phys.* **1984**, *55*, 1492−1507.

(21) Jones, B. A.; Facchetti, A.; Wasielewski, M. R.; Marks, T. J. *J. Am. Chem. Soc.* **2007**, *129*, 15259−15278.

(22) Chang, Y.-C.; Kuo, M.-Y.; Chen, C.-P.; Lu, H.-F.; Chao, I. *J. Phys. Chem. C* **2010**, *114*, 11595−11601.

(23) Newman, C. R.; Frisbie, C. D.; da Silva Filho, D. A.; Brédas, J.-L.; Ewbank, P. C.; Mann, K. R. *Chem. Mater.* **2004**, *16*, 4436−4451.

(24) Rienstra-Kiracofe, J. C.; Tschumper, G. S.; Schaefer, H. F., III; Nandi, S.; Ellison, G. B. *Chem. Rev.* **2002**, *102*, 231−282.

(25) Seguy, I.; Jolinat, P.; Destruel, P.; Mamy, R.; Allouchi, H.; Courseille, C.; Cotrait, M.; Bock, H. *ChemPhysChem* **2001**, *7*, 448−452.

(26) SAINT, Bruker AXS, 1997−2008.

(27) *CrysAlisPro*, Agilent Technologies XRD Products, Yarnton, UK, 2011.

(28) (a) Sheldrick, G. M., SADABS, Bruker AXS, 2004−2008. (b) Sheldrick, G. M., TWINABS, Bruker AXS, 2008.

(29) Blessing, R. H. *Acta Crystallogr.* **1995**, *A51*, 33−38.

(30) (a) Burla, M. C.; Caliandro, R.; Camalli, M.; Carrozzini, B.; Cascarano, G. L.; L. De Caro, Giacovazzo, C.; Polidori, G.; Spagna, R. SIR2004, CNR IC, Bari, Italy, 2004; (b) Burla, M. C.; Caliandro, R.; Camalli, M.; Carrozzini, B.; Cascarano, G. L.; De Caro, L.; Giacovazzo, C.; Polidori, G.; Spagna, R. *J. Appl. Crystallogr.* **2005**, *38*, 381−388.

(31) (a) Sheldrick, G. M. SHELXD, University of Göttingen and Bruker Nonius 2000−4. (b) Sheldrick, G. M.; Hauptman, H. A.; Weeks, C. M.; Miller, R.; Usón, I. Ab initio phasing. In Rossmann, M. G., Arnold, E., Eds.; *International Tables for Crystallography*; IUCr and Kluwer Academic Publishers: Dordrecht, 2001; Vol. *F*, pp 333−351.

(32) Sheldrick, G. M. *Acta Crystallogr.* **2008**, *A64*, 112−122.

(33) (a) Beurskens, P. T.; Beurskens, G.; R. de Gelder, Smits, J. M. M.; S. Garcia-Granda, Gould, R. O. DIRDIF-2008, Radboud University Nijmegen: The Netherlands, 2008. (b) Beurskens, P. T.. In Sheldrick, G. M., C. Krüger, Goddard, R., Eds. *Crystallographic Computing 3*; Clarendon Press: Oxford, UK, 1985; p 216.

(34) (a) Palatinus, L. SUPERFLIP; EPF: Lausanne, Switzerland, 2007. (b) Palatinus, L.; Chapuis, G. *J. Appl. Crystallogr.* **2007**, *40*, 786−790.

(35) Sheldrick, G. M. SHELXL-97, University of Göttingen, 1997.

(36) Sluis, P. v. d.; Spek, A. L. *Acta Crystallogr.* **1990**, *A46*, 194.

(37) (a) Spek, A. L. PLATON, Utrecht University, The Netherlands. (b) Spek, A. L. *J. Appl. Crystallogr.* **2003**, *36*, 7−13.